Comparison of Different Grating Structure DFB Lasers for High-speed Electro-absorption Modulated Lasers

Siti Sulikhah[1], San-Liang Lee[1] and Hen-Wai Tsao[2]
[1]*Department of Electronic and Computer Engineering, National Taiwan University of Science and Technology, Taipei 10607, Taiwan*
[2]*Department of Electrical Engineering, National Taiwan University, Taipei 10607, Taiwan*

Keywords: Electro-absorption Modulator, Optical Interconnect, Partial Grating, Quarter-Wave-Shifted, Uniform Grating.

Abstract: High-speed electro-absorption modulated lasers (EMLs) with three DFB laser structures (uniform grating (UG), asymmetric quarter-wave-shifted (QWS), and partially corrugated grating (PCG)) are investigated here under 56-Gb/s NRZ signal modulation. It is known that the former UG-EML suffers from performance degradation due to the residual facet reflection (RFR) and facet phase fluctuation. PCG-EML with 300-µm long laser section, 175-µm long grating section, 100-µm long modulator section, and 10^{-3} front-facet reflectivity can produce about ~83.8% dynamic single-mode yield (SMY), improved average Q-value, and reduced low-frequency drop (LFD) in the modulation response. By choosing the optimal grating length for the PCG-DFB and applying an asymmetric QWS-DFB, the EMLs can maintain good static- and dynamic performances over a wide range of the linear gain coefficients.

1 INTRODUCTION

According to the upcoming standards authorization of 800G and 1.6T Ethernet, it enforces a huge connectivity requirements for datacentre traffic, especially it is expected to grasp for about 20.6-ZB by year 2021 (Li and Gu, 2019; Spyropoulou et al, 2020; Ambrosia, 2021). Advanced high-speed electro-absorption modulated lasers (EMLs) with augmented immunity to residual facet reflection (RFR) are known as promising candidates for empowering high-capacity optical networking and their applications are expanding from long distance transmission (Ozolins et al, 2017; Pukhrambam et al, 2017). Several groups have reported such ultra-high data rate modulations of EMLs and recently Sumitomo Electric Device Innovations Inc. has developed the packaged EML with a net bit rate of 348.62-Gb/s at 1310.9-nm wavelength for PAM-8 transmission with 55-GHz bandwidth (Hossain et al, 2021). Table 1, the key issues of high-speed EML research and performance, is listed (Kobayashi et al, 2009; Kwon et al, 2012; Cheng et al, 2014; Ohata et al, 2020; Abbasi et al, 2017; Ahmad et al, 2019; Yamauchi et al, 2021).

Trend on ideal design of EML, which is formed with an integrated DFB laser and EAM, involves the laser cavity structure development to provide a robust and reliable light sources for data communication links. Table 2 shows the overview of various DFB laser structures that implement into EML design (Tsuyoshi, 2012), especially standard uniform grating (UG), asymmetric quarter-wave-shifted (QWS), and partially corrugated grating (PCG). Moreover, the schematic diagrams comparison and their average longitudinal power distribution under static condition with laser length of 300-µm are depicted in Figure 1 and Figure 2, respectively.

Table 1: High-speed EML research and performance.

Group	Year	Device Structure & Performance
NTT Corp.	2009	1.55-µm InGaAlAs EML (40-Gb/s)
KAIST	2012	1310-nm EAM-DFB (40-Gb/s)
OPTIMUS	2014	1.55-µm EML array (4x25-Gb/s)
Mitsubishi Electric Corp.	2015	1.3-µm EML (53.2-Gb/s)
Acreo Swedish ICT AB	2017	1.5-µm DFB-TWEAM (>100-GHz)
Ghent Univ.	2017	1.5-µm EAM-III-V-on-Silicon DFB (56-Gb/s)
NCU	2019	1.3-µm EML based SAG (38-GHz)
Lumentum Inc.	2021	1310-nm EAM-DFB (53-Gbaud/s PAM-4)
Sumitomo Elect. Dev. Inn. Inc.	2021	1310.9-nm EML (402-Gb/s PAM-8)

Sulikhah, S., Lee, S. and Tsao, H.
Comparison of Different Grating Structure DFB Lasers for High-speed Electro-absorption Modulated Lasers.
DOI: 10.5220/0010996600003121
In *Proceedings of the 10th International Conference on Photonics, Optics and Laser Technology (PHOTOPTICS 2022)*, pages 172-178
ISBN: 978-989-758-554-8; ISSN: 2184-4364

Table 2: Overview of various DFB laser structures for EML design.

Parameter	UG-DFB	QWS-DFB	PCG-DFB
Integration	-	-	Waveguide
Facet coating	HR/AR	AR/AR or HR/AR	HR/AR
Short active region (<200-µm)	Difficult	Difficult	Easy
Fabrication cost	Medium	High	Low
Butt-joint regrowth	No	No	Yes
Threshold gain	Medium	High	Medium
Single-mode yield	Low	Good	Good

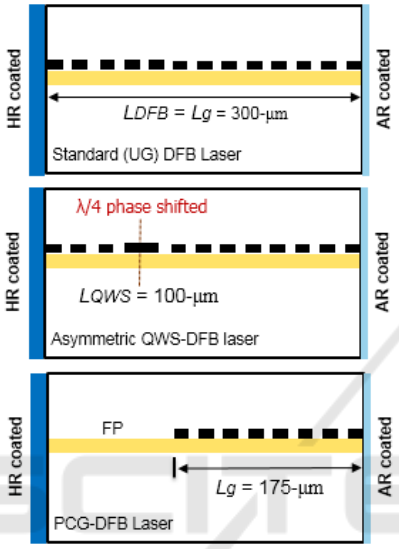

Figure 1: Schematic diagrams of standard UG-DFB (top), asymmetric QWS-DFB (middle), and PCG-DFB (bottom).

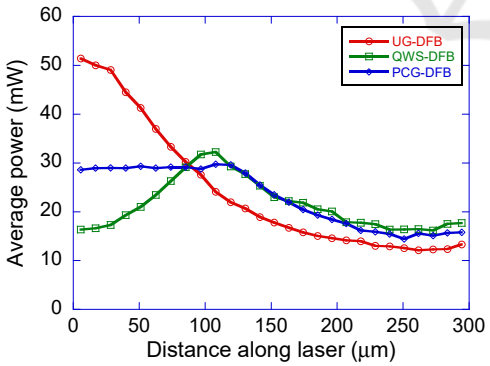

Figure 2: Average longitudinal power distribution comparison of different DFB laser structures.

In our preceding work, EMLs with partial corrugated grating type DFB laser (PCG-EML) was verified by simulation to have better single-mode yield (SMY) and be immune to RFR than the original UG-DFB based EML. The former UG-EML has relatively poor resistance to RFR that can cause output waveform distortion. On the other hand, PCG-EMLs can produce better performance due to laser stability and be approximately invulnerable to the change of reflection from modulator facet (Sulikhah et al, 2019, 2020, 2021). Noticing that if the performance enhancement by PCG-EML can be kept for higher data rate and the election of an optimal grating length (around 60% of DFB laser section) depends on the linear gain coefficient (Huang, 1996, 1998, 1999). Furthermore, an asymmetric QWS-DFB structure with HR-AR coatings was demonstrated to have a better tolerance againts optical feedback as well as good mode selectivity compared to the conventional symmetric QWS-DFB with AR-AR coatings even though the fabrication process is more complicated for a phase-shifted by e-beam writing scemes (Zheng, 2014; Utaka, 1986).

In this research, we focused to design and analyze the comparison of EMLs with UG-DFB, asymmetric QWS-DFB, and PCG-DFB which can extend their applications to a flatten intensity modulation (IM) responses and the higher performance systems. A new approach is proposed by optimizing grating section parameters for 56-Gb/s EML. Both static- and dynamic performances are evaluated with VPIcomponentMaker Photonics Circuits tool, which is very mature scientific and technological direction for end-to end photonics design (e.g., cost-optimized equipment configuration). This time-dependent transmission line laser model (TLLM) allows an efficient simulation of the full dynamics of multi-section semiconductor devices with different grating types and waveguide parameters, including their spectral dynamic (VPIsystem Inc., 2019). It also accounts for the forward and backward propagating waves inside the laser as well as for the spatial hole burning effect from non-uniform carrier and light distribution inside the laser cavity (Lowery, 1989).

2 DEVICE MODELING

Figure 3 shows the schematic diagram of EML with standard UG-DFB (top), asymmetric QWS-DFB (middle), and PCG-DFB (bottom), where the DFB section and EAM section lengths is 300-µm and 100-µm, respectively. For asymmetric QWS-EML, its laser section having a λ/4 phase shifted at 1/3 of DFB laser length (L_{QWS} = 100-µm), while PCG type DFB consists of an uncorrugated waveguide near the HR rear facet and a corrugated grating (L_g = 175-µm) near the EAM facet. The values of the key laser parameters used in evaluating static- and dynamic performances of EMLs are summarized in Table 3. The laser gain

material involves a typical MQW structure operating at 1310-nm wavelength. The DFB laser is biased with a DC current of 70-mA. To investigate the impacts of RFR, the modulator is modulated by 56-Gb/s PRBS-NRZ pattern with 0.5 V voltage swing and a reverse bias voltage of -1 V. The peak absorption wavelength is set as 1281-nm.

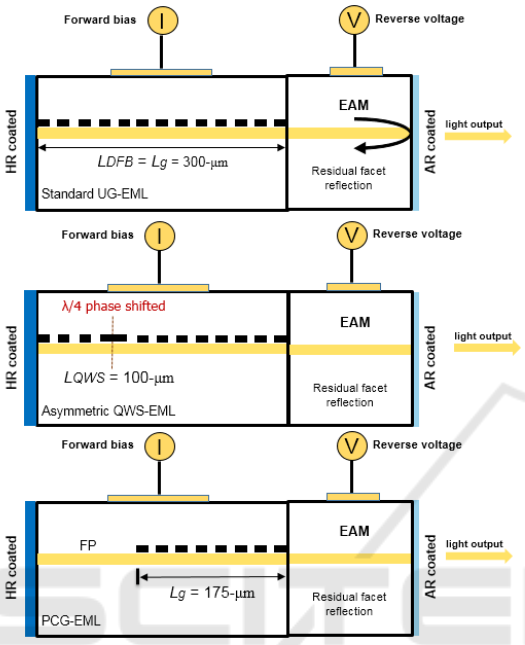

Figure 3: The cross-sectional schematic diagram of EML with standard UG-DFB (top), asymmetric QWS-DFB (middle), and PCG-DFB (bottom).

Table 3: List of device parameters for EML with various DFB laser structures.

Parameter	Value
DFB section length	300 μm
Active region width	1.8 μm
Active region depth of MQW	0.03 μm
Confinement factor of MQW	0.075
Grating coupling strength	5000 m^{-1}
Gain compression factor	$2.5x10^{-23}$ m^3
Internal loss	25 cm^{-1}
Group index	3.73
Injection efficiency	0.75
Transparent carrier density	$1.5x10^{24}$ m^{-3}
Linewidth enhancement factor	3
Gain Model of EAM	
Shape	Lorentzian
EAM length	100 μm
Peak absorption	$1.1x10^5$ m^{-1}
Peak absorption linear	$5.4x10^5$ 1/Vm
Peak absorption quadratic	$1.51x10^6$ $1/V^2m$
Peak absorption cubic	$4.4x10^5$ $1/V^3m$
Peak absorption frequency	234.025 THz
Peak absorption frequency linear	2.12 THz
Absorption bandwidth	3.82 THz
Absorption bandwidth linear	-2.56 THz/V
Saturation carrier density	$5x10^{24}$ m^{-3}

Figure 4 depicts the light-current (L-I) curve of EML with three different DFB structures, where a threshold current of ≥12-mA is exhibited. The comparison value of static extinction ratio (SER) of the modelled EAM has been presented in Figure 5 with SER of >5.52-dB, which has a good fit with the experimental data (dashed line). The results offer similar static characteristics for all various DFB lasers and only slightly different results can be observed by UG-EML.

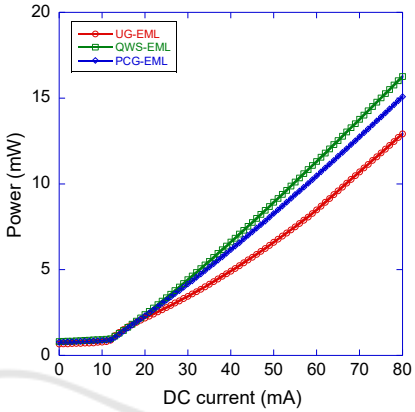

Figure 4: L-I curves of EMLs with various DFB laser structures.

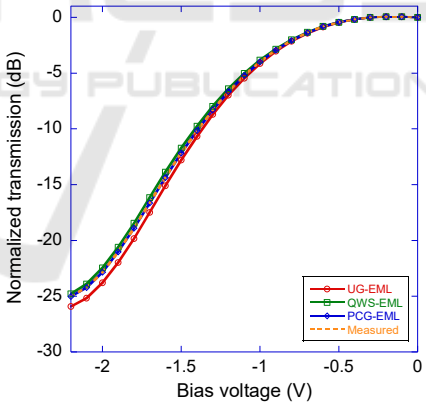

Figure 5: Static extinction ratios comparison of EMLs with various DFB laser structures with rear facet = 0°. Dashed line is measured curve of typical EML.

3 DETAILED DEVICE PERFORMANCES

The effects of linear gain coefficient on static SMY and on average side-mode suppression ratio (SMSR) for EMLs with various DFB laser structures under rear facet phase variation from 0 to 2π are shown in

Figure 6 and Figure 7, accordingly. In general, asymmetric QWS-EML could provide better static SMY (>91.89%) and average static SMSR (>43.34-dB) than PCG-EML with different linear gain coefficients. In contrast, UG-EML shows a clear difference that these two DFB types, whereas only achieve <72.97% SMY with average static SMSR of <40.5-dB. Noting that the SMY is defined as the percentage of phase that the laser can have >35-dB SMSR, set that the phase variation is uniformly distributed between 0 and 2π.

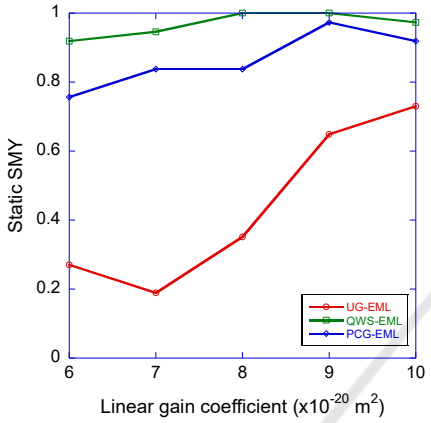

Figure 6: Effect of linear gain coefficient on static single-mode yield for EMLs with various DFB laser structures under 10^{-3} RFR.

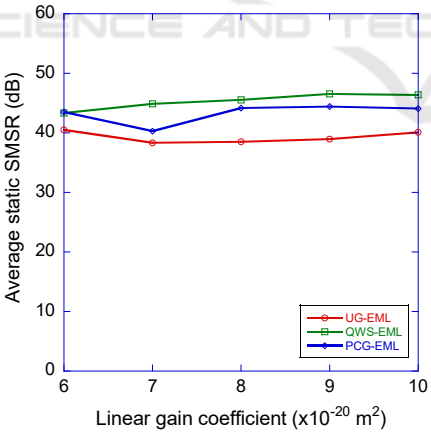

Figure 7: Effect of linear gain coefficient on average static SMSR for EMLs with various DFB laser structures under 10^{-3} RFR.

Then, we compare the simulated dynamic SMY (Figure 8) and average dynamic SMSR (Figure 9) under 56-Gb/s NRZ signal with different linear gain coefficients. From the simulations, UG-EML is sensitive to the change in facet phases, which is persistent with the previous findings of worse resistance to external reflection for UG-DFBs (Grillot and Thedrez, 2006). Moreover, both asymmetric QWS-EML and PCG-EML can have for about the same average dynamic SMSR (~39.8-dB), but asymmetric QWS-EML could obtain a higher dynamic SMY (89.19%) compared to PCG-EML, where the SMY are gradually increased for larger linear gain coefficient.

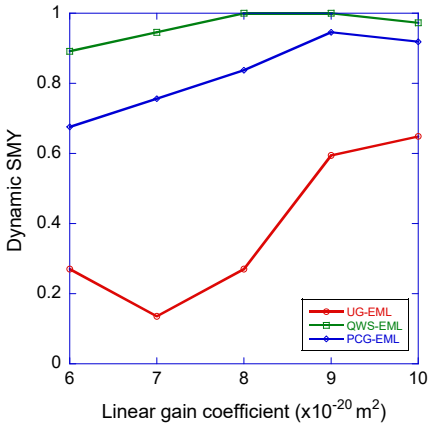

Figure 8: Effect of linear gain coefficient on dynamic single-mode yield for EMLs with various DFB laser structures under 10^{-3} RFR.

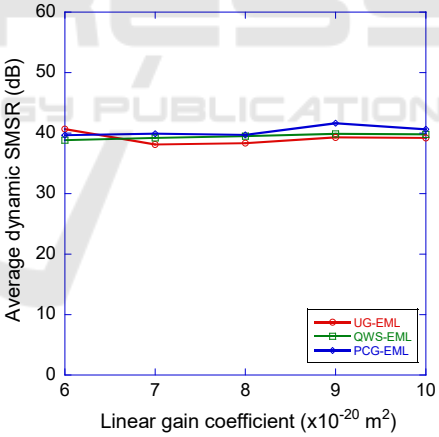

Figure 9: Effect of linear gain coefficient on average dynamic SMSR for EMLs with various DFB laser structures under 10^{-3} RFR.

The simulated eye diagrams under 56-Gb/s NRZ signal for EMLs with various DFB laser structures is shown in Figure 10 with linear gain coefficient of $6x10^{-20}$ m^2, rear facet of 290°, and 10^{-3} reflectivity. The Q-value of UG-EML, asymmetric QWS-EML, and PCG-EML is 5.45, 10.12, and 15.06, respectively. That is, the relative phase between rear facet and gratings incredibly affect the output waveform since it is susceptible to the optical

feedback induced fluctuation in field distributions. Hence, the improved immunity to RFR for PCG-EML results from the insensitivity to the HR facets thus better eye diagrams against the EML with asymmetric QWS-DFB and UG-DFB. The detailed comparison of simulated average quality factor for both PCG-EML and asymmetric QWS-EML with different linear gain coefficients under 10^{-3} reflectivity is shown in Figure 11, which is extracted from eye diagrams under 56-Gb/s NRZ signal. PCG-EML could produce a slightly better average Q-value (>20.8), which is about the same performance with the asymmetric QWS-EML when linear gain coefficient = $10x10^{-20}$ m^2.

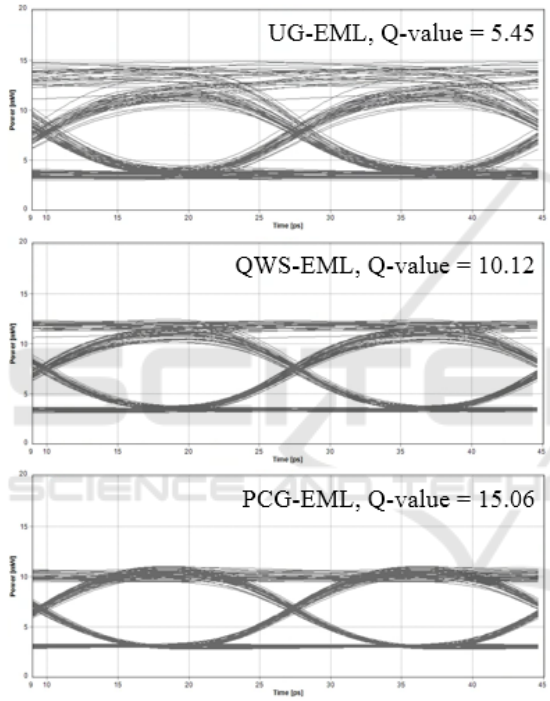

Figure 10: Eye diagrams at 56-Gb/s NRZ signal UG-EML (top), asymmetric QWS-EML (middle), and PCG-EML (bottom) with rear facet = 290°.

Figure 12 depicts the S21 measurement of typical PCG-EML with various bias voltages, which discloses no big difference between PCG-EML, UG-EML, and asymmetric QWS-EML. The 3-dB bandwidth of the EML can be >40-GHz, whereas the transitions of the relaxation oscillation from the peak to dip (i.e., low-frequency drop (LFD)) can be seen in the IM response of EMLs occurred at about 5-GHz. Furthermore, we investigate the simulated intensity modulation responses for three different structures of UG-EML, asymmetric QWS-EML, and PCG-EML with rear facet of 30°. The LFD analyses for different bias voltages are summarized in Table 4. As depicted in Figure 13, both PCG-EML and asymmetric QWS-EML can have a comparable LFD results, whereas QWS-EML produces a better result for some operating bias voltages, especially under 10^{-3} RFR. On the other hand, UG-EML provides more negative LFD, which means more influenced by RFR, compared the two other lasers. Based on these results, both PCG-DFB and asymmetric QWS structures implement a potential candidate in designing high-speed transceivers with robust reliability against the conventional EML with uniform grating. The integrated views of the next requirements of datacentre call for the new architectures based on optical interconnects.

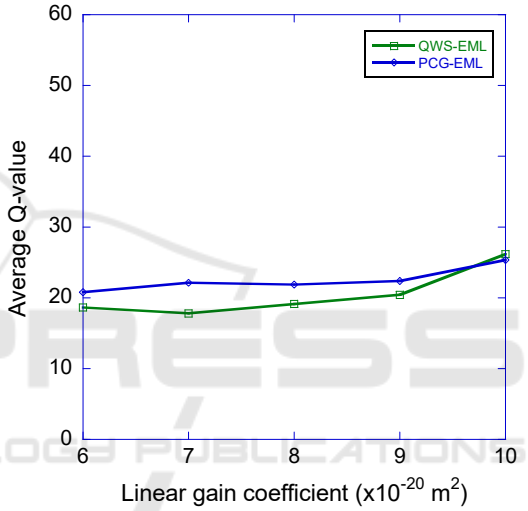

Figure 11: Comparison of simulated average quality factor between PCG-EML and asymmetric QWS-EML with different linear gain coefficients at 56-Gb/s NRZ signal under 10^{-3} RFR.

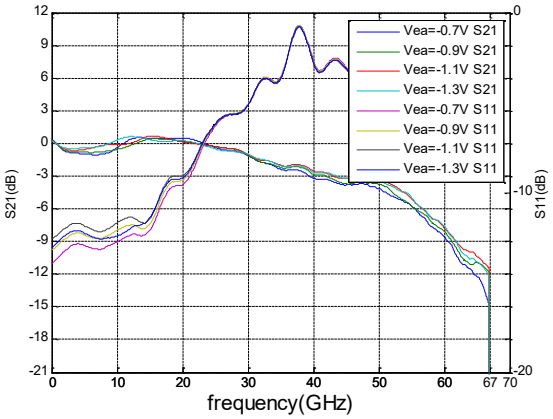

Figure 12: S21 and S11 of typical EML with various bias voltages.

Table 4: LFD analyses for different EML structures.

Bias Voltage (V)	UG-EML	QWS-EML	PCG-EML
-0.8	1.6 dB	-0.8 dB	-0.4 dB
-1	-2.7 dB	-0.6 dB	-0.8 dB
-1.2	1.4 dB	-0.2 dB	-0.5 dB
-1.4	-0.4 dB	-0.1 dB	-0.2 dB
-1.6	-1 dB	-0.1 dB	-0.1 dB
-1.8	-0.4 dB	-0.2 dB	-0.6 dB

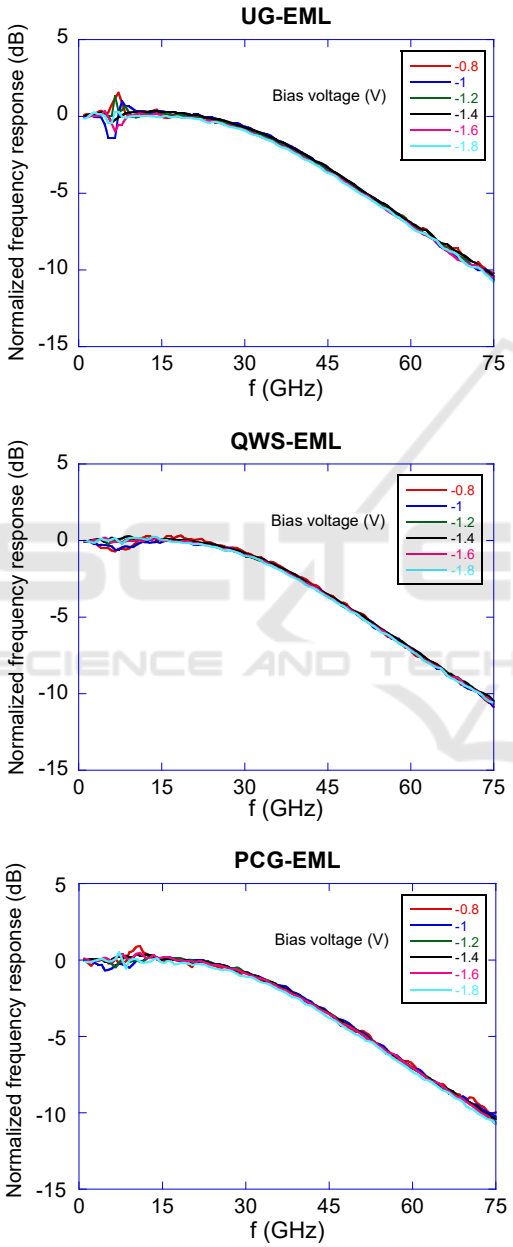

Figure 13: The simulated intensity modulation responses for UG-EML (top), asymmetric QWS-EML (middle), and PCG-EML (bottom) with rear facet = 30°.

4 CONCLUSIONS

We have successfully demonstrated and investigated the performance comparison of EMLs with three different DFB laser structures. The simulation suggests that both asymmetric quarter-wave-shifted and partially corrugated grating based EMLs could provide a better dynamic single-mode yield of 89.19% compared to conventional EML with uniform grating (<64.87% dynamic SMY), but PCG-EML produces a better average Q-value of >20.8 at 56-Gb/s NRZ signal against the two other lasers even with strong reflection from the front section. It also indicates lower low-frequency drop for two types of EMLs with asymmetric QWS-DFB and PCG-DFB (>-0.8 dB) than the original UG-EMLs (-2.7 dB). Therefore, PCG-DFB with HR/AR structure provides a better choice for low-cost and high-speed EML applications.

ACKNOWLEDGEMENTS

The authors would like to thank the Ministry of Science and Technology (MOST), Taiwan for their financial support for this work under the grant number MOST 109-2622-E-011-001-CC1.

REFERENCES

Li, X., Gu, Q. (2019). High-speed on-chip light sources at the nanoscale. *Advances in Physics*, *4*(1), 761-769.

Spyropoulou, M. et al (2020). Towards 1.6T datacentre interconnect technologies: The TWILIGHT perspective. *Journal of Physics Photonics*, *2*(4), 1-5.

Ambrosia, J.D. (2021). The case for 1.6 Terabit Ethernet. In *IEEE 802.3 Beyond 400 Gb/s Ethernet Study Group Electronic May 2021 Session*.

Ozolins, O. et al (2017). 100 GHz externally modulated laser for optical interconnects. *Journal of Lightwave Technology*, *35*(6), 1174-1179.

Pukhrambam, P.D. et al (2017). Electroabsorption modulated lasers with immunity to residual facet reflection by using lasers with partially corrugated gratings. *IEEE Photonics Journal*, *9*(2), 1-17.

Hossain, M.S.B. et al (2021). 402 Gb/s PAM-8 IM/DD O-band EML transmission. In *European Conference on Optical Communication*. Bordeaux, France.

Kobayashi, W. et al (2009). 40-Gbit/s, uncooled (-15 to 80°C) operation of a 1.55-μm, InGaAlAs, electroabsorption modulated laser for very short reach applications. In *IEEE International Conference on Indium Phospide & Related Materials*. Newport Beach, CA, USA.

Kwon, O.K. et al (2012). Electroabsorption modulated laser with high immunity to residual facet reflection. *IEEE Journal of Quantum Electronics*, *48*(9), 1203-1213.

Cheng, Y. et al (2014). 1.55 μm high speed low chirp electroabsortion modulated laser arrays based on SAG scheme. *Optics Express*, *22*(25), 31286-31292.

Ohata, N. et al (2020). High-speed optical devices and packaging techniques for data centers. In *SPIE OPTO*. San Francisco, CA, USA.

Abbasi, A. et al (2017). Direct and electroabsorption modulation of a III-V-on-Silicon DFB laser at 56 Gb/s. *IEEE Journal of Selected Topics in Quantum Electronics*, *23*(6), 1-7.

Ahmad, Z. et al (2019). High-speed electro-absorption modulated laser at 1.3 μm wavelength based on selective area growth technique. In *IEEE Photonics Conference*. San Antonio, TX, USA.

Yamauchi, S. et al (2021). 224-Gb/s PAM4 uncooled operation of lumped-electrode EA-DFB lasers with 2-km transmission for 800GbE application. In *Optical fiber Communication Conference*. San Francisco, CA, USA.

Tsuyoshi, T. (2012). High-speed directly modulated lasers. In *The National Fiber Optic Engineers Conference*. Los Angeles, CA, USA.

Sulikhah, S. et al (2019). Enhancement of modulation responses of directly modulated lasers with passive feedback and partially corrugated grating. In *24th Microoptics Conference*. Toyama, Japan.

Sulikhah, S. et al (2020). Demonstration of improved immunity to residual facet reflection for uncooled EMLs with partially corrugated grating. In *Optoelectronics and Communications Conference*. Taipei, Taiwan.

Sulikhah, S. et al (2021). Improvement on direct modulation responses and stability by partially corrugated gratings based DFB lasers with passive feedback. *IEEE Photonics Journal*, *13*(1), 1-15.

Huang, Y. et al (1996). External optical feedback resistant characteristics in partially-corrugated-waveguide laser diodes. In *Optical Fiber Communication Conference*. San Jose, CA, USA.

Huang, Y. et al (1998). High-yield external optical feedback resistant partially-corrugated-waveguide laser diodes. In *IEEE 16th International Semiconductor Laser Conference*. Nara, Japan.

Huang, Y. et al (1999). External optical feedback resistant 2,5-Gb/s transmission of partially corrugated waveguide laser diodes over a −40 °C to 80 °C temperature range. *IEEE Photonics Technology Letters*, *11*(11), 1482-1484.

Zheng, J. et al (2014). An equivalent-asymmetric coupling coefficient DFB laser with high output efficiency and stable single longitudinal mode operation. *IEEE Photonics Journal*, *6*(6), 1-10.

Utaka, K. et al (1986). λ/4-shifted InGaAsP/InP DFB lasers. *IEEE Journal of Quantum Electronics*, *22*(7), 1113-1114.

(2019). *VPIcomponentMaker 10.0 Photonic Circuit User's Manual*, VPIsystems Inc. Somerset, NJ, USA.

Lowery, A.J. (1989). New dynamic multimode model for external cavity semiconductor lasers. *IEEE Proc. J. Optoelectronics, 136*(4), 229-237.

Grillot, F, Thedrez, B.J. (2006). Facet phase effects on the coherence collapse threshold of 1.55 μm AR/HR distributed feedback semiconductor lasers. In *SPIE Photonics Europe*. Strasbourg, France.